Magnetized quark matter with a magnetic-field dependent coupling

Chang-Feng Li, Li Yang,[1] Xin-Jian Wen,[1,*] and Guang-Xiong Peng[2,3,†]

[1]*Department of Physics and Institute of Theoretical Physics, Shanxi University, Taiyuan 030006, China*
[2]*College of Physics, University of Chinese Academy of Sciences, Beijing 100049, China*
[3]*Synergetic Innovation Center for Quantum Effects and Application, Hunan Normal University,*
Changsha 410081, China

It was recently derived that the QCD running coupling is a function of the magnetic field strength under the strong magnetic field approximation. Inspired by this progress and based on the self-consistent solutions of gap equations, the properties of two-flavor and three-flavor quark matter are studied in the framework of the Nambu–Jona-Lasinio model with a magnetic-field-dependent running coupling. We find that the dynamical quark masses as functions of the magnetic field strength are not monotonous in the fully chirally broken phase. Furthermore, the stability of magnetized quark matter with the running coupling is enhanced by lowering the free energy per baryon, which is expected to be more stable than that of the conventional constant coupling case. It is concluded that the magnetized strange quark matter described by running coupling can be absolutely stable.

I. INTRODUCTION

The properties of strongly interacting quark matter under a strong magnetic field have attracted much attention in the last decade [1]. The structure of dense matter and the behavior of the interaction coupling constant will provide a new clue to the comprehensive understanding of QCD theory under extreme conditions [2]. It has been proposed theoretically and experimentally that a strong magnetic field could be present in the core of neutron stars and in the noncentral collision experiments in the Relativistic Heavy Ion Collider or the Large Hadron Collider [3]. The typical strength of the strong magnetic fields could be of the order of 10^{12} gauss on the surface of pulsars. Some magnetars can have even larger magnetic fields as high as 10^{16} gauss [4]. By comparing the magnetic and gravitational energies, the physical upper limit to the total neutron star is of order 10^{18} gauss. And for the self-bound quark stars, the limit could go higher [5]. The maximum strengths of $10^{18} \sim 10^{20}$ gauss in the interior of stars are proposed by an application of the viral theorem [3,6]. At the LHC/CERN energy, it is estimated to produce a field as large as 5×10^{19} gauss [3,7]. It is thus reasonable to assume a uniform and constant magnetic field to mimic the environment of the chiral phase transition in heavy-ion collisions [8–11]. The important effects on the quark matter led by the strong magnetic field mainly include the following two aspects. First, the strong magnetic field produces the magnetic catalysis on the chiral phase transition at finite temperature. Second, the charged fermions ruled by the Landau level will display an anisotropic structure with respect to the

direction of the magnetic field. In fact, the behavior of quark matter is mainly related to the quark condensate subject to the strong magnetic field [11]. Consequently, the interaction potential and the QCD ground state will be affected by the magnetic field [12,13].

As is well known, the running behavior of the QCD coupling with densities reflects the essential properties of strongly interacting matter, which can be shown by solving the renormalization group (RG) equation. In a strong magnetic field, the RG equation and the polarization tensor will change due to the fact that charged particles in a magnetic field obey the Pauli exclusion rule and the Landau energy level arrangement [14,15]. Therefore, the magnetic-field-dependent coupling has been proposed and verified recently [11,14,16]. Until now, the effect of the magnetic-field dependence has been studied by several versions of the analytic parametrization formula $\alpha_s(eB)$ [11,14,17]. The investigation of the effect of the magnetic field on the coupling constant can be summarized by two trends. One is to present an analytic function of the running behavior at ultra-strong magnetic field. The theoretical derivation of the magnetic-field-dependent running coupling and the effective fermion mass in the propagator can be obtained by the Schwinger-Dyson equation in the one-loop approximation. The other is to fit the general parametrization relation between the coupling constant and the magnetic field in order to reproduce the critical temperature of the chiral symmetry breaking from lattice QCD, since there is no direct result of the running constant as a function of the magnetic field.

In the literature, the Nambu–Jona-Lasinio (NJL) model has been widely employed in the study of the stability properties of strange quark matter (SQM) without a magnetic field [18–20]. Recently, the NJL model has been

*[*]wenxj@sxu.edu.cn
[†]gxpeng@gucas.ac.cn

extended to the case of a strong magnetic field and many special properties due to the magnetic field, for example, the (inverse) magnetic catalysis effect [21]. It is certainly expected that the stability of SQM is also strongly affected by the magnetic field through the coupling constant. In previous work using the NJL model, it was shown that a spherical droplet of color-flavor locked (CFL) quark matter has a larger gap energy when the coupling constant increases. A larger gap energy will lead to lower free energy. Therefore, it is possible to find absolutely stable CFL strangelets for a coupling constant G larger than some critical value [22]. However, the magnetic field will rule out the constraint on the coupling constant [23]. Namely, a droplet of magnetized quark matter may exist for any value of G. In the quasiparticle model, we also roughly found that for a proper value the magnetic field can enhance the stability of the quark matter [24]. In the present paper, we analyze the dynamical masses and the stability of quark matter with the field-dependent running coupling in the NJL model.

The paper is organized as follows. In Sec. II, we present the thermodynamics of the NJL model under a strong magnetic field. The thermodynamical treatments in both SU(2) and SU(3) versions are shown in the two subsections, respectively. In Sec. III, the numerical results for the two-flavor and three-flavor quark matter in β equilibrium are presented, and the discussions are focused on the stability properties and the thermodynamical effect of the magnetic-field-dependent running coupling. The last section is a short summary.

II. THERMODYNAMICS AND STABILITY OF MAGNETIZED QUARK MATTER

The dynamics of QCD matter are affected by strong magnetic fields, especially with a magnitude of $eB \sim 15m_\pi^2 (\sim 10^{19}$ gauss) that can be produced in noncentral relativistic heavy-ion collisions. In this paper, we mimic the environment by assuming a uniform magnetic field in the z direction, i.e., $A_\mu = \delta_{\mu 2} x_1 B$. First, we focus on the two-flavor quark matter in the SU(2) NJL model. Then we continue to study SQM in the SU(3) model.

A. SU(2) NJL model in a strong magnetic field

In the SU(2) version of the NJL model in a strong magnetic field, the Lagrangian density reads

$$\mathcal{L}_{\text{NJL}} = \bar{\psi}(i\slashed{D} - m)\psi + G[(\bar{\psi}\psi)^2 + (\bar{\psi}i\gamma_5\vec{\tau}\psi)^2], \quad (1)$$

where ψ represents a flavor isodoublet (u and d quarks). The coupling of the quarks to the electromagnetic field is introduced by the covariant derivative $D_\mu = \partial_\mu - iq_{\text{f}}A_\mu$. Since the model is not renormalizable at zero temperature, we should introduce a cutoff Λ in the 3-momentum space as in the usual way that has been modified by a density-dependent momentum cutoff [20]. Considering the general

graphics of the dynamical fermion mass generation in the Hartree (mean-field) approximation [25], the dynamical quark mass entering the thermodynamic potential at finite chemical potential with a strong magnetic field is related to the condensation term as

$$M_i = m_i - 2G\langle\bar{\psi}\psi\rangle, \quad (2)$$

where the condensation is $\langle\bar{\psi}\psi\rangle = \sum_{i=u,d}\phi_i$ for the two-flavor case. The constituent mass of flavor i depends on both condensates. Therefore, we can always get the same mass $M_u = M_d = M$, even for different charges and chemical potentials. The contribution from the quark flavor i is

$$\phi_i = \phi_i^{\text{vac}} + \phi_i^{\text{mag}} + \phi_i^{\text{med}}. \quad (3)$$

The terms ϕ_i^{vac}, ϕ_i^{mag}, and ϕ_i^{med} representing the vacuum, magnetic field, and medium contribution to the quark condensation are, respectively [10],

$$\phi_i^{\text{vac}} = -\frac{MN_c}{2\pi^2}\left[\Lambda\sqrt{\Lambda^2 + M^2} - M^2\ln\left(\frac{\Lambda + \sqrt{\Lambda^2 + M^2}}{M}\right)\right], \quad (4)$$

$$\phi_i^{\text{mag}} = -\frac{M|q_i|BN_c}{2\pi^2}\left\{\ln[\Gamma(x_i)] - \frac{1}{2}\ln(2\pi) + x_i - \frac{1}{2}(2x_i - 1)\ln(x_i)\right\}, \quad (5)$$

$$\phi_i^{\text{med}} = \sum_{k_i=0}^{k_{i,\text{max}}} a_{k_i}\frac{M|q_i|BN_c}{2\pi^2}\ln\left[\frac{\mu_i + \sqrt{\mu_i^2 - s_i^2}}{s_i}\right]. \quad (6)$$

The effective quantity $s_i = \sqrt{M^2 + 2k_i|q_i|B}$ sensitively depends on the magnetic field. The dimensionless quantity is $x_i = M^2/(2|q_i|B)$. The degeneracy label of the Landau energy level is $a_{k_i} = 2 - \delta_{k0}$. The quark condensation is greatly strengthened by the factor $|q_iB|$ together with the dimension reduction $D - 2$ [14,26]. The Landau quantum number k_i and its maximum $k_{i,\text{max}}$ are defined as

$$k_i \leq k_{i,\text{max}} = \text{Int}\left[\frac{\mu_i^2 - M^2}{2|q_i|B}\right], \quad (7)$$

where "Int" means the number before the decimal point.

The total thermodynamic potential density in the mean-field approximation is

$$\Omega = \frac{(M - m_0)^2}{4G} + \sum_{i=u,d}(\Omega_i^{\text{vac}} + \Omega_i^{\text{mag}} + \Omega_i^{\text{med}}), \quad (8)$$

where the first term in the summation is the vacuum contribution to the thermodynamic potential, i.e.,

$$\Omega_i^{\mathrm{vac}} = \frac{N_c}{8\pi^2}\left[M^4\ln\left(\frac{\Lambda+\epsilon_\Lambda}{M}\right)-\epsilon_\Lambda\Lambda(\Lambda^2+\epsilon_\Lambda^2)\right], \quad (9)$$

where the quantity ϵ_Λ is defined as $\epsilon_\Lambda = \sqrt{\Lambda^2+M^2}$. The ultraviolet divergence in the vacuum part of the thermodynamic potential Ω is removed by the momentum cutoff. In the literature, a form factor is introduced in the diverging zero energy as a smooth regularization procedure [27]. The magnetic field and medium contributions are, respectively,

$$\Omega_i^{\mathrm{mag}} = -\frac{N_c(|q_i|B)^2}{2\pi^2}\left[\zeta'(-1,x_i)-\frac{1}{2}(x_i^2-x_i)\ln(x_i)+\frac{x_i^2}{4}\right], \quad (10)$$

$$\Omega_i^{\mathrm{med}} = -\frac{|q_i|BN_c}{4\pi^2}\sum_{k=0}^{k_{\max}}a_{k_i}\left\{\mu_i\sqrt{\mu_i^2-(M^2+2k_i|q_i|B)}\right.$$
$$\left. -(M^2+2k_i|q_i|B)\ln\left[\frac{\mu_i+\sqrt{\mu_i^2-(M^2+2k_i|q_i|B)}}{\sqrt{M^2+2k_i|q_i|B}}\right]\right\}, \quad (11)$$

where $\zeta(a,x) = \sum_{n=0}^{\infty}\frac{1}{(a+n)^x}$ is the Hurwitz zeta function. From the thermodynamic potential (25), one can easily obtain the quark density as

$$n_i(\mu, B) = \sum_{k=0}^{k_{i,\max}}a_{k_i}\frac{|q_i|BN_c}{2\pi^2}\sqrt{\mu_i^2-(M^2+2k_i|q_i|B)}. \quad (12)$$

The relevant pressure from the flavor i contribution is

$$P_i(\mu_i, B) = -\Omega_i = -(\Omega_i^{\mathrm{vac}}+\Omega_i^{\mathrm{mag}}+\Omega_i^{\mathrm{med}}). \quad (13)$$

Under strong magnetic fields, the system's total pressure should be a sum of the matter pressure and the field pressure contributions [10,28]. So we have

$$P_i(\mu_i, B) = -\Omega_i + \frac{B^2}{2}, \quad (14)$$

where the magnetic field term $B^2/2$ is due to the electromagnetic Maxwell contribution. It is well known to us that the energy density and pressure should vanish in vacuum. So the pressure and the thermodynamic potential should be normalized by requiring zero pressure at zero density as [10]

$$P_i^{\mathrm{eff}}(\mu_i, B) = P_i(\mu_i, B) - P_i(0, B). \quad (15)$$

In the normalization result, the field term is automatically absent. According to the fundamental thermodynamic relation, the free energy density at zero temperature is

$$\varepsilon_i = -P_i^{\mathrm{eff}} + \mu_i n_i. \quad (16)$$

For asymmetric quark matter we should impose the β equilibrium by including the electron contribution under strong magnetic fields. The electron chemical potential is not independent an variable and can be expressed by the quark chemical potentials as $\mu_e = \mu_d - \mu_u$. According to the similar normalization procedure in Eq. (15), it is required that $P_{e,\mathrm{eff}} = P_e(\mu_e, B) - P_e(\mu_e, 0)$. So the pressure of electrons can be simplified as $P_e^{\mathrm{eff}} = -\Omega_e^{\mathrm{med}}$ by setting $N_c = 1$ and $M = m_e$ in Eq. (11). The corresponding number density and the energy density are

$$n_e(\mu_e, B) = \sum_{k=0}^{k_{e,\max}}a_{k_i}\frac{|eB|}{2\pi^2}\sqrt{\mu_e^2-(m_e^2+2k|eB|)}, \quad (17)$$

$$\varepsilon_e = -P_e^{\mathrm{eff}} + \mu_e n_e. \quad (18)$$

For the stellar matter in β equilibrium, the charge neutrality condition is

$$2n_u - n_d - 3n_e = 0. \quad (19)$$

The system pressure and energy density are written as

$$P = \sum_i P_i^{\mathrm{eff}}, \qquad \varepsilon = \sum_i \varepsilon_i, \quad (20)$$

where the summation goes over u, d quarks and electrons.

The interaction coupling constant between quarks should in principle be solved by the RG equation, or it can be phenomenologically expressed in an effective potential [29–31]. In the infrared region at low energy, the dynamical gluon mass represents the confinement feature of QCD [32]. Furthermore, in the presence of a strong magnetic field, the gluon mass becomes large together with a decreasing of the interaction constant, which leads to the damping of chiral condensation. For sufficiently strong magnetic fields $eB \gg \Lambda_{\mathrm{QCD}}^2$, the coupling constant α_s is proposed to be related to the magnetic field as [11,14]

$$\alpha_s(eB) = \frac{12\pi}{(11N_c-2N_f)\ln(|eB|/\Lambda_{\mathrm{QCD}}^2)}. \quad (21)$$

Motivated by the work of Miransky and Shovkovy [14], a similar ansatz of the magnetic-field-dependent coupling constant was introduced in the SU(2) NJL [17] and SU(3) NJL models [11]. In the two-flavor version of the NJL model, based on the lattice simulations, an interpolating formula was proposed as [17]

$$G'(eB) = \frac{G}{1+\alpha\ln(1+\beta|eB|/\Lambda_{\mathrm{QCD}}^2)}, \quad (22)$$

where the energy scale is $\Lambda_{\mathrm{QCD}} = 200$ MeV. The parameters $\alpha = 2$ and $\beta = 0.000327$ are from the fit of the lattice

result for quarks condensates [17]. We can find that the running coupling constant versus the field B gradually approaches the constant value $G'(B \to 0) \sim G$.

B. Magnetized strange quark matter in the SU(3) NJL model

The SU(3) NJL Lagrangian density includes both a scalar-pseudoscalar interaction and the 't Hooft six-fermion interaction [23] and can be written as [33]

$$\mathcal{L}_{\mathrm{NJL}} = \bar{\psi}(i\slashed{D} - m)\psi + G \sum_{a=0}^{8} [(\bar{\psi}\lambda_a\psi)^2 + (\bar{\psi}\gamma_5\lambda_a\psi)^2]$$
$$- K\{\det_f[\bar{\psi}(1+\gamma_5)\psi] + \det_f[\bar{\psi}(1-\gamma_5)\psi]\}. \quad (23)$$

The field $\psi = (u, d, s)^T$ represents a quark field with three flavors. Correspondingly, $m = \mathrm{diag}(m_u, m_d, m_s)$ is the current mass matrix with $m_u = m_d \neq m_s$. $\lambda_0 = \sqrt{2/3}I$, where I is the unit matrix in the three-flavor space. λ_a with $0 < a \leq 8$ denotes the Gell-Mann matrix. Compared with the two-flavor case, the gap equations for the three-flavor case are coupled and should be solved consistently,

$$M_i - m_i + 4G\phi_i - 2K\phi_j\phi_k = 0, \quad (24)$$

where (i, j, k) is the permutation of (u, d, s). The quark condensates are the same as in Eq. (3).

The total thermodynamic potential density in the mean-field approximation reads

$$\Omega = 2G \sum_{i=u,d,s} \phi_i^2 - 4K\phi_u\phi_d\phi_s$$
$$+ \sum_{i=u,d,s} (\Omega_i^{\mathrm{vac}} + \Omega_i^{\mathrm{mag}} + \Omega_i^{\mathrm{med}}). \quad (25)$$

The corresponding calculations of the normalized pressure and energy density are similar to the SU(2) model.

The simple ansatz of the running coupling is probably suitable for the SU(3) NJL model if we include the s quarks [11],

$$G'(eB) = \frac{G}{\ln(e + |eB|/\Lambda_{\mathrm{QCD}}^2)}, \quad (26)$$

where the parameter $\Lambda_{\mathrm{QCD}} = 300$ MeV, which is different from the value in Eq. (22).

III. NUMERICAL RESULT AND DISCUSSION

A. Symmetric and asymmetric SU(2) quark matter

In the computation of this subsection, we consider the following set of parameters for the SU(2) NJL model [34]: $\Lambda = 587.9$ MeV, $N_c = 3$, $m_u = m_d = 5.6$ MeV, and $G = 2.44/\Lambda^2$. The corresponding electric charges are $|q_d| = |q_s| = 1/3 = |q_u|/2$ in units of the elementary

charge. First, we investigate the symmetric quark matter with a common chemical potential μ and common dynamical quark mass $M(\mu, eB)$ and do the calculation under the coupling constant G and the magnetic-field-dependent running coupling $G'(eB)$ in Eq. (22). The dynamical quark mass can be determined by the gap equation (2). It should be noticed that the gap equation has more than one solution, with the physical being the one that minimizes the thermodynamic potential. The zero chemical potential case is the fully chirally broken phase. In Fig. 1, we show the dynamical quark mass $M(0, eB)$ as a function of magnetic field strength B. The solid curve is for the fixed coupling constant G. An increase of the magnetic field leads to an enhancement of the quark mass, which reflects the so-called magnetic catalysis. The dashed curve is for the case of the running coupling $G'(eB)$. It shows the distinct behavior of the effective mass versus the magnetic field. In particular, by comparing the case of the coupling constant it is clear that the running coupling constant $G'(eB)$ produces an inverse behavior of the dynamical mass in the magnetic field range of $10^{17} \sim 10^{19}$ gauss. In the chiral-symmetry-broken phase, the quark effective mass will feel the influence of the magnetic field through the correction to the quark propagator. The numerical result in Fig. 1 shows that the characteristic becomes more apparent for the magnetic field $B = 10^{19}$ gauss, where the running coupling sensitively depends on the magnetic field. But for smaller values of the magnetic field, the two curves will gradually move closer to each other due to the asymptotic behavior of the running coupling constant $G'(eB \to 0) \sim G$, where the coupling nearly remains invariant.

For the massive phase with nonzero chemical potential at the magnetic field $B = 2 \times 10^{19}$ gauss, we can solve the gap equation and calculate the dynamical quark mass
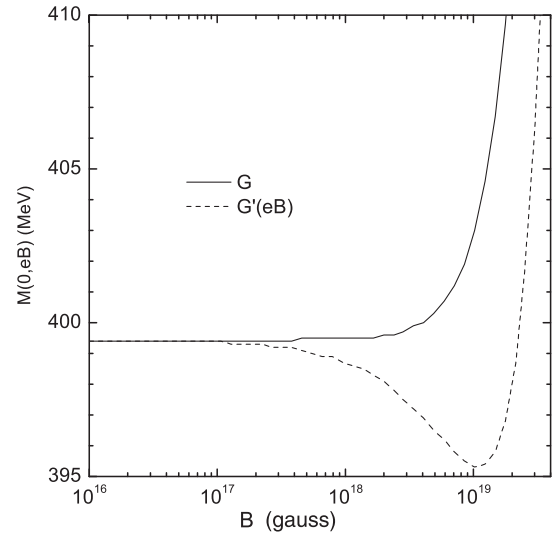

FIG. 1. Dynamical quark mass of SU(2) quark matter in the fully chirally broken phase as a function of B for the fixed coupling constant G and the running coupling $G'(eB)$.
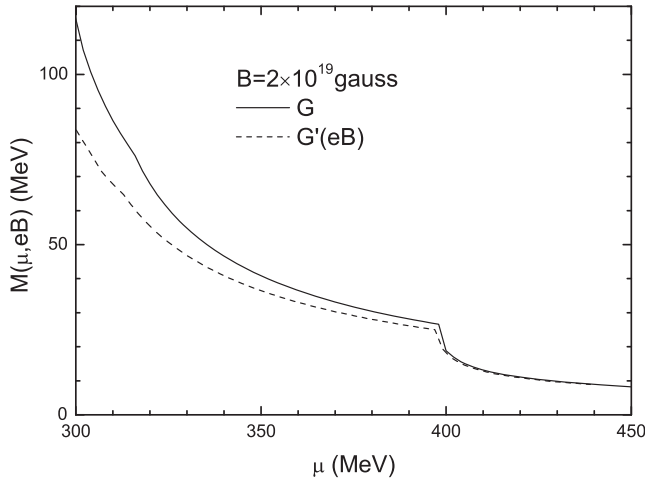
FIG. 2. Dynamical quark mass in the massive phase as a monotonous decreasing function of the chemical potential for the couplings G and $G'(eB)$.

$M(\mu, eB)$, which is dependent on both the chemical potential and the given magnetic field. In Fig. 2, it is shown that the dynamical quark mass will decrease as the chemical potential increases. The quark mass under the running coupling $G'(eB)$ is lower than that of the fixed coupling constant G case, which is more clear in the small chemical potential region. It shows that the correction of the running coupling constant becomes very important near the infrared region. Correspondingly, the free energy per baryon versus the baryon number density is shown in Fig. 3. The free energy with the running coupling $G'(eB)$ is marked by the dashed curve, which is lower than that of the fixed coupling case marked by the solid curve. The value of the minimum of the free energy per baryon on both curves is much bigger than the average energy value 930 MeV for ^{56}Fe. So it demonstrates that the two-flavor quark matter is
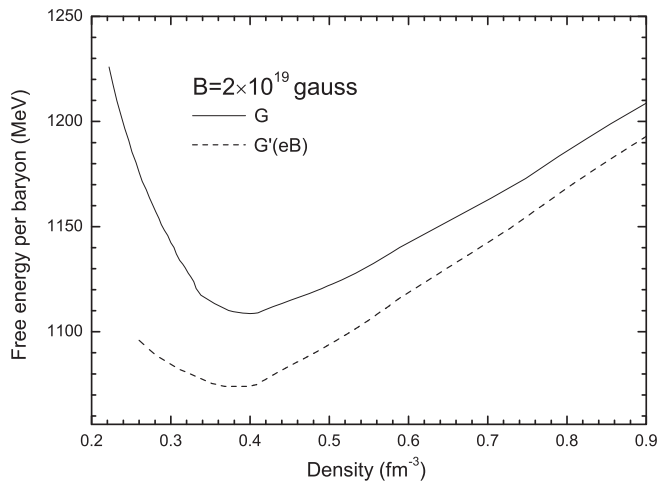
less stable than nuclear matter [35], which is in agreement with the Witten-Bodmer hypothesis [36].

Now we study the isospin-symmetric quark matter by setting the common chemical potential for u and d quarks. The isospin symmetry can be broken under a strong magnetic field because of the charge splitting for different flavors. We suppose that the quark matter reaches the β equilibrium condition. So the chemical potentials satisfy $\mu_u + \mu_e = \mu_d$. The dynamic masses and the two independent chemical potentials (μ_u, μ_d) can be self-consistently solved by three equations: the gap equation (2), the baryon number conservation, and the charge neutrality condition (19). In Fig. 4 the asymmetric chemical potentials are shown at the magnetic field $B = 2 \times 10^{19}$ gauss. The appearance of the inflection points on the curves is due to the contribution of the Landau level. The d quark chemical potential μ_d is always much bigger than that of the u quark. In fact, it is naturally required that the number of d quarks is larger than the number of u quarks in order to reach global electrical neutrality together with the small amount of leptons. On the other hand, it is understood that the Landau level of the d quark could be more than the u quark level.

In Fig. 5, the free energy per baryon versus the baryon number density is shown for different magnetic fields. The minimum of the free energy per baryon is in the zero-pressure state. From top to bottom, the magnetic fields of the three curves are, respectively, $B = 1 \times 10^{18}$, 8×10^{18}, and 2×10^{19} gauss. It is known that the degeneracy factor of the quark condensation is proportional to the magnetic field, so there will be more quarks accommodated in the lowest Landau level for a larger magnetic field. This is the reason why the quark matter will have lower free energy at a stronger magnetic field. A larger magnetic field will enhance the stability of quark matter by lowering the free energy per baryon. Furthermore, we can find that the free

FIG. 3. The free energy per baryon of the symmetric quark matter versus the baryon number density for the same parameter sets as Fig. 2.
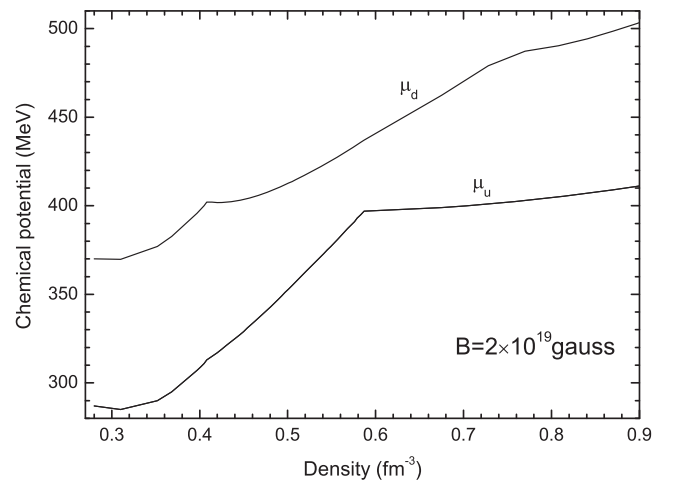

FIG. 4. The quark chemical potential versus the baryon number density for the asymmetric quark matter at $B = 2 \times 10^{19}$ gauss.
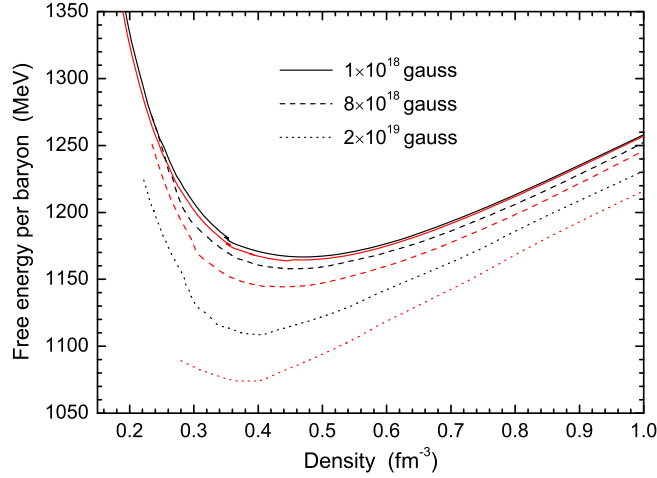
FIG. 5. The free energy per baryon of the asymmetry two-flavor quark matter versus the baryon number density at the three different magnetic field values. The three red curves are for the running coupling $G'(eB)$.

energy at the running coupling $G'(eB)$ (marked by red curves) is all lower than that of the coupling constant G at the same field B.

B. Numerical results of the SU(3) NJL model

It is necessary to extend the study of the stability of magnetized quark matter to the SU(3) case. For the SU(3) NJL model, we adopt the parameters $\Lambda = 602.3$ MeV, $m_u = m_d = 5.5$ MeV, $m_s = 140.7$ MeV, $G = 1.835/\Lambda^2$, and $K = 12.36/\Lambda^5$ [37]. We assume that the three-flavor quark matter is in β equilibrium. Now there are three dynamical masses and two independent chemical potentials, which can be determined by the three gap equations (24), the baryon number conservation, and the neutral charge condition,

$$2n_u - n_d - n_s - 3n_e = 0. \qquad (27)$$

In the fully chirally broken phase at zero chemical potential, the dynamical quark masses only depend on the magnetic field. In Fig. 6, we show the dynamical quark masses of three flavors as functions of the magnetic field. The dashed, dotted, and solid curves are, respectively, for the u, d, and s quarks. The corresponding red ones represent the quark masses at the running coupling $G'(eB)$ in Eq. (26). As in the SU(2) case, the running coupling produces different behavior for the dynamical masses for all three flavors.

We can solve the dynamical masses $M_i(\mu, eB)$ at finite chemical potential in Fig. 7. The dynamical masses of u and d quarks apparently decrease as the density increases. At the coupling constant $G = 2 \times 10^{19}$ gauss, M_s almost remains a constant of 466 MeV or so. Consequently, the strange quarks have no real distribution in its Landau level

in the system. On the contrary, the running coupling $G'(eB)$ will lead to smaller dynamical masses (marked by red curves). The strange quark mass M_s decreases slightly as the density increases, and thus the lowest Landau level of the strange quark can appear at least. In Fig. 8, we compare the free energy per baryon under different coupling cases at the same magnetic field $B = 2 \times 10^{19}$ gauss. The upper solid curve is for the coupling constant G and the lower dashed curve is for the running coupling $G'(eB)$.
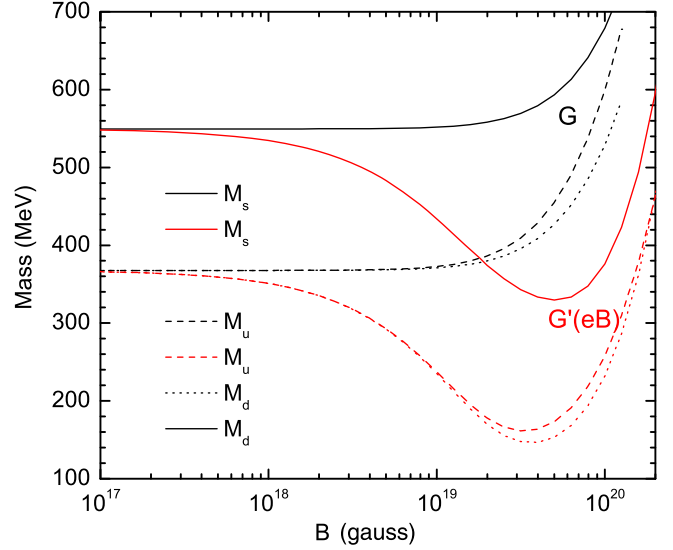

FIG. 6. Dynamical quark masses in the three-flavor quark matter as functions of B in the fully chirally broken phase. The solid, dashed, and dotted curves from top to bottom denote the masses M_s, M_u, and M_d, respectively. The red curves are for the running coupling case.
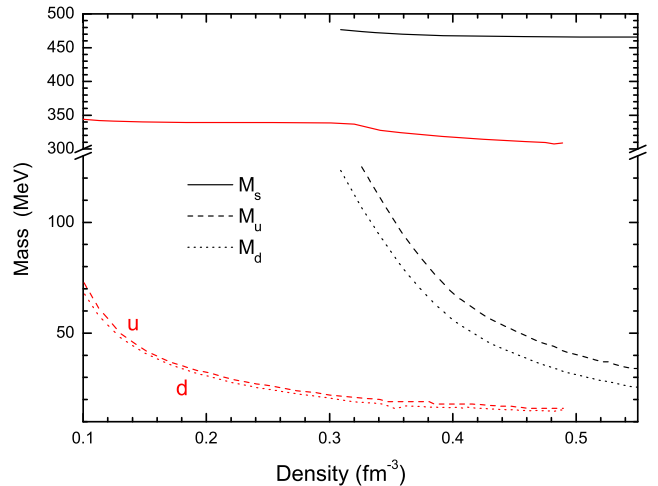

FIG. 7. Dynamical quark masses in the three-flavor quark matter as functions of the baryon number density at the magnetic field $B = 2 \times 10^{19}$ gauss. The curves from top to bottom denote M_s, M_u, and M_d, respectively. The red curves are for the running coupling case.
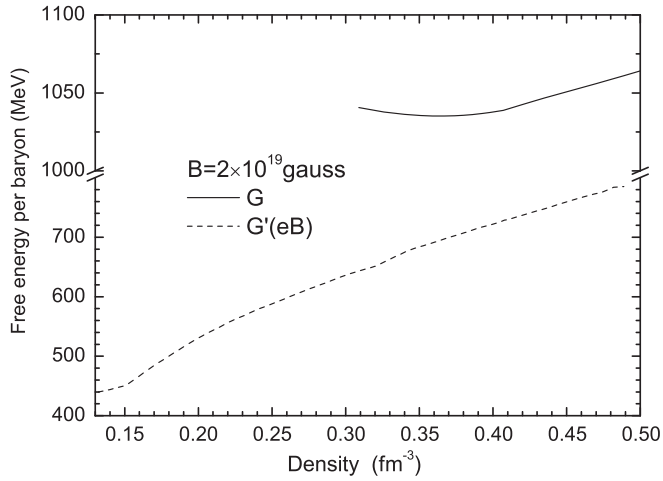
FIG. 8. The free energy per baryon of the three-flavor quark matter versus the baryon number density at the magnetic field strength $B = 2 \times 10^{19}$ gauss.

Therefore, it is possible that the strange quark matter with a running coupling in a proper magnetic field could be absolutely stable.

IV. SUMMARY

We have studied the magnetized quark matter in the NJL model with a magnetic-field-dependent running coupling to reflect the magnetic field effect on the QCD vacuum structure and the interaction potential between quarks. The effect becomes more important in the infrared region. We studied the thermodynamic properties of both the two-flavor and three-flavor quark matter in β equilibrium under a strong magnetic field.

In the NJL model, a magnetic field changes the quark dynamical mass by modifying the quark condensation in the gap equations. In the computation, we solved the gap equations for the fixed coupling G and the magnetic-field-dependent running coupling $G'(eB)$, respectively. First, in the fully chirally broken phase, we found that the dynamical quark mass as only a function of the magnetic field is not monotonous, contrary to the previous result for the conventional fixed coupling constant. Furthermore, for two-flavor quark matter in a larger magnetic field (about 10^{19} gauss), the running coupling $G'(eB)$ leads to a sharp drop of the dynamical mass as the magnetic field increases, and a similar behavior appears for three-flavor quark matter for a higher magnetic field than that of the two-flavor case. Due to the reduction of the dynamical mass, the strange quarks have a real distribution in the lowest Landau energy level at least. Second, we found that the free energy per baryon of the symmetric quark matter is smaller than that of the asymmetric case, and it will decrease as the magnetic field strength increases. Furthermore, we found that the stability of the magnetized quark matter in β equilibrium can be enhanced under the running coupling by lowering the free energy. So the magnetized SQM could be absolutely stable with the running coupling. In fact, the comprehensive understanding of the QCD running coupling is meaningful together with the one-loop vacuum and quark-gluon vertex correction in the presence of a strong magnetic field [38], which will greatly affect the chiral phase transition and the stability properties of quark matter in a strong magnetic field. The strong magnetic field will inevitably lead to the anisotropic magnetization and pressure with respect to the direction of the field [39,40]. It is expected that the field-dependent coupling would play a role in the anisotropic structure and phase transition, which will be studied in the future.

[1] V. A. Miransky and I. A. Shovkovy, Phys. Rep. **576**, 1 (2015).

[2] M. Buballa, Phys. Rep. **407**, 205 (2005).

[3] D. E. Kharzeev, L. D. McLerran, and H. J. Warringa, Nucl. Phys. **A803**, 227 (2008); V. V. Shokov, A. Y. Illarionov, and V. D. Toneev, Int. J. Mod. Phys. A **24**, 5925 (2009).

[4] C. Thompson and R. C. Duncan, Astrophys. J. **473**, 322 (1996).

[5] G. Chanmugam, Annu. Rev. Astron. Astrophys. **30**, 143 (1992); D. Lai, Rev. Mod. Phys. **73**, 629 (2001).

[6] L. Dong and S. L. Shapiro, Astrophys. J. **383**, 745 (1991).

[7] V. Voronyuk, V. D. Toneev, W. Cassing, E. L. Bratkovskaya, V. P. Konchakovski, and S. A. Voloshin, Phys. Rev. C **83**, 054911 (2011).

[8] P. G. Allen and N. N. Scoccola, Phys. Rev. D **88**, 094005 (2013).

[9] J. K. Boomsma and D. Boer, Phys. Rev. D **81**, 074005 (2010).

[10] D. P. Menezes, M. B. Pinto, S. S. Avancini, A. P. Martínez, and C. Providência, Phys. Rev. C **79**, 035807 (2009); S. S. Avancini, D. P. Menezes, and C. Providência, Phys. Rev. C **83**, 065805 (2011); M. Ferreira, P. Costa, D. P. Menezes,

C. Providência, and N. N. Scoccola, Phys. Rev. D **89**, 016002 (2014).

[11] M. Ferreira, P. Costa, O. Lourenco, T. Frederico, and C. Providência, Phys. Rev. D **89**, 116011 (2014).

[12] M. A. Andreichikov, V. D. Orlovsky, and Y. A. Simonov, Phys. Rev. Lett. **110**, 162002 (2013).

[13] E. J. Ferrer, V. de la Incera, I. Portillo, and M. Quiroz, Phys. Rev. D **89**, 085034 (2014).

[14] V. A. Miransky and I. A. Shovkovy, Phys. Rev. D **66**, 045006 (2002).

[15] E. J. Ferrer, V. de la Incera, and A. Sanchez, Phys. Rev. Lett. **107**, 041602 (2011).

[16] E. J. Ferrer, V. de la Incera, and X. J. Wen, Phys. Rev. D **91**, 054006 (2015).

[17] R. L. S. Farias, K. P. Gomes, G. Krein, and M. B. Pinto, Phys. Rev. C **90**, 025203 (2014).

[18] M. Asakawa and K. Yazaki, Nucl. Phys. **A504**, 668 (1989).

[19] M. Buballa, Nucl. Phys. **A611**, 393 (1996); I. N. Mishustin, L. M. Satarov, H. Stocker, and W. Greiner, Phys. Rev. C **62**, 034901 (2000).

[20] M. Baldo, G. F. Burgio, P. Castorina, S. Plumari, and D. Zappalà, Phys. Rev. C **75**, 035804 (2007).

[21] K. G. Klimenko, Z. Phys. C **54**, 323 (1992); V. P. Gusynin, V. A. Miransky, and I. A. Shovkovy, Phys. Rev. Lett. **73**, 3499 (1994); E. J. Ferrer and V. de la Incera, Phys. Lett. B **481**, 287 (2000); N. Mueller and J. M. Pawlowski, Phys. Rev. D **91**, 116010 (2015).

[22] O. Kiriyama, Int. J. Mod. Phys. A **21**, 3021 (2006).

[23] K. G. Klimenko and D. Ebert, Phys. At. Nucl. **68**, 124 (2005).

[24] X. J. Wen, Phys. Rev. D **88**, 034031 (2013).

[25] C. Ratti, Europhys. Lett. **61**, 314 (2003); M. Buballa and M. Oertel, Phys. Lett. B **457**, 261 (1999).

[26] T. Kojo and N. Su, Nucl. Phys. **A931**, 763 (2014).

[27] R. Gatto and M. Ruggieri, Phys. Rev. D **82**, 054027 (2010); S. Yasui and A. Hosaka, Phys. Rev. D **74**, 054036 (2006).

[28] J. L. Noronha and I. A. Shovkovy, Phys. Rev. D **76**, 105030 (2007). E. J. Ferrer, and V. de la Incera, Lect. Notes Phys. **871**, 399 (2013); L. Paulucci, E. J. Ferrer, V. de la Incera, and J. E. Horvath, Phys. Rev. D **83**, 043009 (2011).

[29] J. L. Richardson, Phys. Lett. B **82**, 272 (1979).

[30] M. Sinha, X.-G. Huang, and A. Sedrakian, Phys. Rev. D **88**, 025008 (2013).

[31] J.-F. Xu, G.-X. Peng, F. Liu, D.-F. Hou, and L.-W. Chen, Phys. Rev. D **92**, 025025 (2015).

[32] A. A. Natale, Nucl. Phys. B, Proc. Suppl. **199**, 178 (2010).

[33] A. G. Grunfeld, D. P. Menezes, M. B. Pinto, and N. N. Scoccola, Phys. Rev. D **90**, 044024 (2014).

[34] T. Hatsuda and T. Kunihiro, Phys. Rep. **247**, 221 (1994).

[35] C.-J. Xia, G.-X. Peng, E.-G. Zhao, and S.-G. Zhou, Science bulletin **61**, 172 (2016); C.-J. Xia, G.-X. Peng, S.-W. Chen, Z.-Y. Liu, and J.-F. Xu, Phys. Rev. D **89**, 105027 (2014).

[36] A. R. Bodmer, Phys. Rev. D **4**, 1601 (1971); E. Witten, Phys. Rev. D **30**, 272 (1984).

[37] P. Rehberg, S. P. Klevansky, and J. Hüfner, Phys. Rev. C **53**, 410 (1996).

[38] A. Ayala, C. A. Dominguez, L. A. Hernández, M. Loewe, and R. Zamora, arXiv:1510.09134.

[39] A. A. Isayev and J. Yang, Phys. Rev. C **84**, 065802 (2011); J. Phys. G **40**, 035105 (2013); E. J. Ferrer, V. de la Incera, J. P. Keith, I. Portillo, and P. L. Springsteen, Phys. Rev. C **82**, 065802 (2010).

[40] D. P. Menezes, M. B. Pinto, and C. Providência, Phys. Rev. C **91**, 065205 (2015).